



2820 East College Avenue, Suite J.
State College, PA 16801
Tel: 814-2387485
Fax: 814-2387539

Final Report for Phase II SBIR titled

“High-Q Tunable Microwave Superconducting Strip-Line Filters”

Contract No. F49620-03-C-0012

Principal Investigator: Dean Anderson

Co-Investigator: Paul Rehrig

TRS Technologies, Inc.
2820 East College, Suite J., State College, PA 16801

Investigators from Sub-contractor

Principal Investigator: Mike Lanagan

Co-Investigators: Eugene Furman, Xiaoxing Xi

Materials Research Institute
Penn State University, University Park, PA 16802

Program Manager:

Dr. Harold Weinstock

April 08, 2005

DISTRIBUTION STATEMENT A

Approved for Public Release

Distribution Unlimited

REPORT DOCUMENTATION PAGE		Form Approved OMB No. 0704-0188	
1. AGENCY USE ONLY (Leave blank)		2. REPORT DATE 14 April 2005	
4. TITLE AND SUBTITLE High-Q Tunable Microwave Superconducting Strip-Line Filters		3. REPORT TYPE AND DATES COVERED Final Technical Report	
6. AUTHOR(S) Dean A. Anderson		5. FUNDING NUMBERS C: F49620-03-C-0012	
7. PERFORMING ORGANIZATION NAME(S) AND ADDRESS(ES) TRS Ceramics, Inc. 2820 East College Avenue State College, PA 16801		8. PERFORMING ORGANIZATION REPORT NUMBER TRS0004Z	
9. SPONSORING/MONITORING AGENCY NAME(S) AND ADDRESS(ES) Department of the Air Force Air Force Office of Scientific Research (AFOSR) 875 North Randolph Street Arlington, VA 22203-1768		10. SPONSORING/MONITORING AGENCY REPORT NO.	
11. SUPPLEMENTARY NOTES			
12A. DISTRIBUTION/AVAILABILITY STATEMENT (If contract specifies restricted distribution, state restriction instead of Unclassified-Unlimited.) Distribution Statement A. Approved for public release; distribution is unlimited.		12b. DISTRIBUTION CODE	
13. ABSTRACT (Maximum 200 words) The objective of the Phase II SBIR project was to develop high Q, tunable microwave filters by using a cryogenic piezoelectric actuator to mechanically tune a high temperature superconducting (HTS) resonator. The concept, designated piezotun-HTS, will enable a broad range of civilian and military applications that require precise band selectivity over a broad frequency range. In Phase I of this project, a 25% frequency tuning range was successfully demonstrated between 2 and 8 GHz by using a piezoelectric bending element to adjust the width of an air gap between a microstrip resonator and a dielectric or metal tuning plate. In Phase II, the piezotune-HTS and strip-line resonator concepts are applied to achieve large tuning range and low insertion loss.			
14. SUBJECT TERMS Cryogenic superconducting actuator Strip-line		15. NUMBER OF PAGES 22	
piezotune-HTS resonator High Q		16. PRICE CODE	
17. SECURITY CLASSIFICATION OF REPORT Unclassified	18. SECURITY CLASSIFICATION OF THIS PAGE Unclassified	19. SECURITY CLASSIFICATION OF ABSTRACT Unclassified	20. LIMITATION OF ABSTRACT SAR

I. Project Objectives: The objective of the Phase II SBIR project was to develop high Q, tunable microwave filters by using a cryogenic piezoelectric actuator to mechanically tune a high temperature superconducting (HTS) resonator. The concept, designated piezotune-HTS, will enable a broad range of civilian and military applications that require precise band selectivity over a broad frequency range. In Phase I of this project, a 25% frequency tuning range was successfully demonstrated between 2 and 8 GHz by using a piezoelectric bending element to adjust the width of an air gap between a microstrip resonator and a dielectric or metal tuning plate. In Phase II, the piezotune-HTS and strip-line resonator concepts are applied to achieve large tuning range and low insertion loss.

I.1 Background

Tunable filters are important elements of the RF front end of frequency-agile radar and communication systems. Currently, there are three major approaches used to tune microwave devices including filters: electric field tunable devices, magnetically tunable, and mechanically induced tuning. Electrically tunable devices, such as the ones based on barium strontium titanate (BST) bulk or thin film forms, are capable of excellent tunability but suffer from the relatively low Q which is limited by microwave losses in the nonlinear dielectric materials used for tuning. In general, tunability and Q is inversely related to each other. Paraelectric thin films, such as BST and SrTiO₃, demonstrate large changes in dielectric constant with applied electric field. However, this only occurs when dielectric constant and loss are relatively high compared to conventional microwave resonator dielectrics. This results in impedance matching problems and large insertion losses. Dielectric bulk ceramic paraelectric materials have better Q values, but at the cost of reduced tunability. In addition, bulk ceramic paraelectrics often require very high tuning voltages (>1000V). Magnetic tuning often suffers from bulky tuning structures, and is limited in frequency range over which tuning can take place. Only modest tunability is offered by tunable cavity structures based on magnetic materials. Tuning speed is another important factor for tuning structure. Paraelectric materials respond very quickly to changes in the electric field and the tuning speed depends upon the power of the external driving circuit. Magnetic tuning can be accomplished on the time scale of 100 ns. In general, the insertion losses for both magnetic and electric tuning increase with increasing frequencies due to increased intrinsic losses in the nonlinear materials. Further known limitation of tuning relying on material nonlinearity is a concern with intermodulation product frequencies potentially distorting filter characteristics. This is especially a concern for high power applications. The advantage of electric and magnetic tuning is fast tuning with tuning times in the range of microseconds is possible.

The conventional mechanical displacement for tuning is one of the oldest tuning techniques and is often used to adjust resonance frequency of a filter. Both metals and dielectrics are used for tuning. Use of high Q dielectric plates for tuning purpose results in a large tuning range and low insertion loss. Conventional mechanical displacement is limited by low tuning bandwidth. The purpose of piezoelectric tuning is to combine advantages of conventional mechanical tuning with increased tuning speed. Piezoelectric tuning is based on the control of impedance and of the effective dielectric constant by means of piezoelectric transducer. This is most commonly accomplished by translating a

dielectric tuning plate in the region of high electric fields. The displacement of dielectric plate by piezoelectric transducer changes effective dielectric constant of the medium resulting in changing speed of wave propagation in composite medium. Piezoelectric tuning approach had been utilized to control delay lines [1], phased arrays [2], bandstop [3] and bandpass [4] filters. Extension of the piezotune technique to high Q HTS filters has always been problematic because of the poor performance of conventional piezoelectrics at cryogenic temperatures. The innovation demonstrated in this work is to use novel single crystal relaxor ferroelectrics for the piezoelectric tuning element. These materials exhibit tremendously large electric field induced strains compared to conventional piezoelectric ceramics as shown in Figure 1, and a significant piezoelectric effect is retained on cooling to cryogenic temperatures [5,6]. The large electric field induced strain in these materials is due to their very large piezoelectric coefficients (see Table I), defined as the linear dependence of strain on electric field

$$\varepsilon_{ij} = d_{ij}E_j \quad (1)$$

where ε_{ij} is the strain tensor

E_j is the electric field (V/m)

d_{ij} is the piezoelectric coefficient in m/V

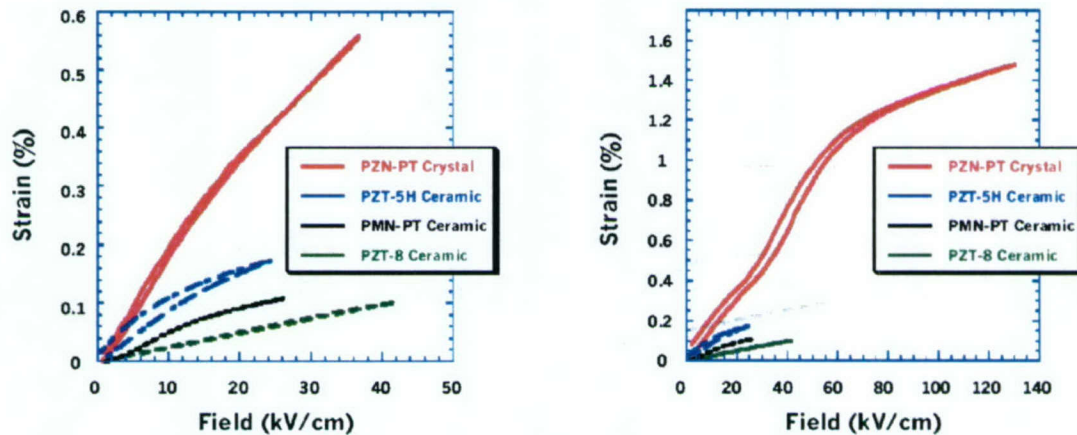


Figure 1. Piezoelectric strain vs. electric field for single crystal ferroelectrics and a variety of piezoelectric ceramics. Left: Strain levels at typical actuator operation fields. Right: very high single crystal strain due to field induced phase transition at high electric field.

Table I: Comparison of Piezoelectric Properties for Single Crystal Ferroelectrics and Typical Ceramic Materials

Property	PMN-PT Crystal Standard Cut	PMN-PT Crystal High d_{31} Cut	Type VI (PZT-5H) Ceramic
Dielectric Constant	8000	---	3900
d_{33} (pm/V)	2250	1116	690
d_{31} (pm/V)	-950	-1632	-340
Y_{33} (GPa)	12	---	47
Y_{11} (GPa)	17	---	60

Piezoelectrics based on ferroelectric ceramics $\text{Pb}(\text{Zr,Ti})\text{O}_3$ (PZT) and crystals must be polarized with a large electric field. This aligns the ferroelectric domains (analogous to ferromagnetic domains) to produce a piezoelectric effect. Piezoelectric positioners or actuators generally make use of either the expansion along the polarization direction when a positive electric field is applied along the same direction (d_{33} coefficient) or the contraction perpendicular to the polarization direction when a positive electric field is applied parallel to the polarization (d_{31} coefficient). Although d_{33} is larger than d_{31} , for positioning applications requiring low force (such as piezoelectric tuning), bending elements, which amplify d_{31} , are an effective means of achieving large displacements. From Table I it can be easily seen that the d_{33} and d_{31} for single crystal PMN-PT is about 3 times the value for the best PZT ceramic. In addition, crystal cuts have recently been discovered which exhibit extremely high d_{31} 's of over 1500 pm/V, almost 5 times the value for PZT. These high coefficients have allowed the fabrication of single crystal piezoelectric actuators with large stroke and low profile.

Because single crystals have such high room temperature piezoelectric coefficients they retain significant piezoelectricity as they are cooled to cryogenic temperatures. The d_{31} and d_{33} coefficient vs. temperature is shown in Figure 2 for single crystal and conventional PZT-based piezoelectrics. At 77K the d_{31} for the crystals is almost 5 times the value for PZT ceramic, and at 20K the crystal piezoelectric effect is still as strong as PZT at room temperature.

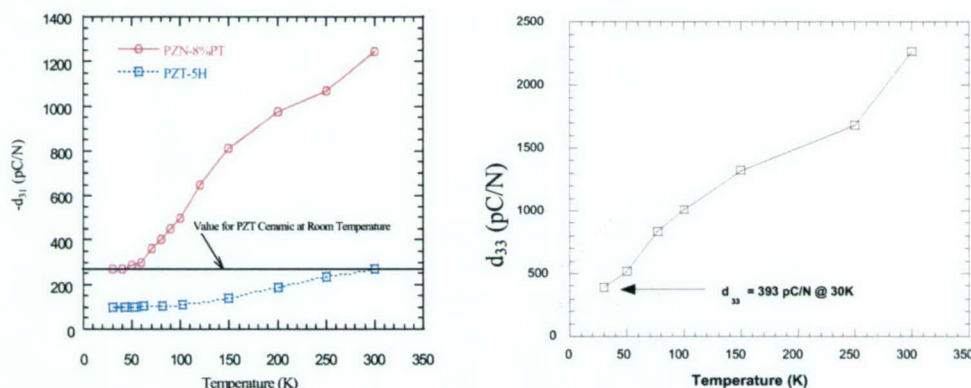


Figure 2. Piezoelectric coefficient vs. temperature for a single crystal piezoelectrics (PZN-PT crystal) and a standard PZT ceramic material.

Insertion loss for frequency agile-tunable filters should be minimized because these losses degrade the system noise figure and dynamic range [7]. Thus it is useful to utilize materials which do not contribute to energy loss in the filter. Superconducting tunable filters are very attractive for these applications because of greatly reduced losses in the electrodes. At 10 GHz, the surface resistance of YBCO superconducting film is lower than that of copper by a factor of 30 and remains below values for copper up to 100 GHz.

In phase 1 of this project we have demonstrated high tunability with both metal and dielectric tuning materials which were used to tune ring resonators on alumina substrates

at room temperature. However, the Q of such devices and insertion losses are not optimized due to energy loss in the conductors printed on alumina substrates and due to high insertion losses of ring resonators. In phase 2 of this project one of the goals was to explore the possibility of combining high tunability achievable with piezoelectric tuning with the low loss superconductor – based filter. The other goal was to characterize horseshoe filters at room temperature as the prototypes of low insertion loss filters that are well tailored for piezoelectric tuning.

1.2 Approaches

On the basis of the success of the Phase I project, electrically tuned microstrip resonator designed by PSU was demonstrated using low profile single crystal piezoelectric actuators. Both “31” mode and “33” mode flexensional single crystal piezoelectric actuators were designed, fabricated and tested at room temperature and cryogenic temperature. With the developed cryogenic piezoelectric actuators, YBCO film based HTS resonators from STI were tuned in liquid nitrogen for high Q tunable HTS filters.

II. Piezo tuned Strip line resonator

II.1 Resonance Tuning Analysis

The perturbation technique is a useful approach in assessing the direction in which resonance frequency shifts with the movement of the tuning plate. There are two types of perturbation: material perturbation and shape perturbation as shown in Figure 3. Both types of perturbation are strictly applicable to a close cavity. However, the trends of changes in frequency with perturbation of resonance conditions are applicable for the planar resonance structures reported here.

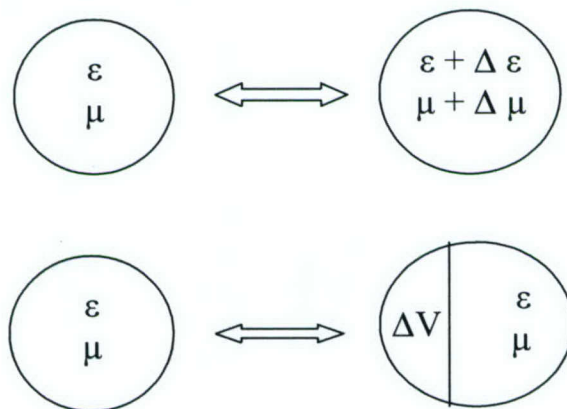


Figure 3. Schematic diagram of material (top) and shape (bottom) perturbations.

A. Material perturbation.

This case is applicable for the introduction of a material with a different dielectric constant or permeability compared to the ones originally present. One common example of material perturbation is use of nonlinear tunable dielectric microwave materials such as BST. Nonlinear magnetic materials have also been used for the purpose of frequency adjustment. An approximation of frequency shift is shown in (2):

$$\frac{\omega - \omega_0}{\omega_0} \cong \frac{- \int_{V_0} (\Delta \epsilon |E_0|^2 + \Delta \mu |H_0|^2) dv}{\int_{V_0} (\epsilon |E_0|^2 + \mu |H_0|^2) dv} \quad (2)$$

Where ω_0 is the unperturbed resonance frequency, ω is the perturbed resonant frequency, $\Delta \mu$ is the change in magnetic permeability of the medium, and $\Delta \epsilon$ is the change in dielectric permittivity of the medium. E_0 and H_0 are unperturbed electric and magnetic fields which are assumed to be approximately the same for the perturbed case.

As one can see from this equation, increase of either ϵ or μ results in a downward shift in resonance frequency. There is also an increase in stored energy for either case. Theoretically, there is no preference for using tunable ϵ or μ for tuning purposes since they affect tunability in exactly the same way. Given a choice, there are advantages in using both for tuning, since a greater control of impedance becomes possible. To test the feasibility of using magnetic materials for tuning purposes, magnetic permeability was increased from one to ten in the finite difference time domain (FDTD) modeling, and consistent with the prediction of equation 1, the resonance frequency shifted downwards.

In the case of horseshoe filters, the design permitted approximately constant impedance as a result of tuning capacitance for both coupled branches of the filter and there was no need to introduce magnetic materials.

B. Shape perturbation.

In addition to tuning resonance frequency as a consequence of shape perturbation, it is also possible to perturb the shape of the cavity to obtain frequency shift. The expression for the frequency shift in the case of cavity perturbation is given in (3):

$$\frac{\omega - \omega_0}{\omega_0} \cong \frac{\int_{\Delta V_0} (\mu |H_0|^2 - \epsilon |E_0|^2) dv}{\int_{V_0} (\epsilon |E_0|^2 + \mu |H_0|^2) dv} \quad (3)$$

The terms in the numerator are proportional to the energy removed by the perturbation compared to the total stored energy given by the denominator. The above equation thus can also be written as (4):

$$\frac{\omega - \omega_0}{\omega_0} \cong \frac{\Delta W_m - \Delta W_e}{W} \quad (4)$$

where W is the total stored energy in the original cavity. Thus the inward perturbation will raise resonant frequency if it is made in the region of large magnetic energy, ΔW_m , compared to the electric energy in the same region, ΔW_e .

Therefore, unlike material perturbation, shape perturbation can result in either upward or downward shift in the resonant frequency. To maximize the shift in the resonance frequency, two conditions should be satisfied: 1). A region with a large difference

between stored magnetic and electrical energy should be used and 2). The magnitude of the stored energy in the perturbed region should be a large fraction of the total stored energy.

In practice, both types of perturbations are used for the tested filters. By bringing the tuning plate close to the resonator, we increase effective dielectric constant by replacing air ($k = 1$) with the plate with $k \gg 1$. The tuning is a consequence of field extending above a filter being nonuniform: by moving plate close to the filter it enters a region of greater stored energy. This material type of perturbation should always lead to the reduction of resonant frequency, which is what we normally observe. For the shape perturbation, the electrical boundary conditions are important: In particular, having a metal electrode in contact with the tuning plate results in shape perturbation which we know can tune resonance frequency in either direction. The metal electrode can be either grounded to define electrical potential or be thicker than the skin depth to effectively reflect the electromagnetic energy at its interface with the dielectric plate. Experimentally, the electroded sample resulted in a greater shift of resonance frequency which is consistent with the shape and material perturbations being additive. Interestingly, in the Phase I of this project we have seen that the metal plate of a specific geometry used without an attached dielectric provided an upward shift in resonant frequency. However, different sized metal plates gave opposite sign of tuning. The effect of metal on tunability is consistent with shape perturbation alone, since the nonmagnetic metal plates were used.

To have a more quantitative understanding of filter behavior we have used finite integral and finite difference time domain modeling. Models indicated that there was only a weak dependence of resonance on whether tuning dielectric plate was connected to ground plane or if it was electroded with the floating potential. Also, thicker tuning plates are predicted to lead to greater tunability. However, in practice use of thick plates lead to the problems of resonance inside the tuning plate and greater inertial mass which can result in slower tuning.

We also modeled the effects of material perturbation alone which mimics tunable BST samples. The model predicted about 10 percent tunability with changes in the dielectric constant of horseshoe capacitors from 100 to 85. This K tunability can be achieved experimentally in MgO doped BST samples. This tuning is less than can be obtained with the piezoelectric tuning and also the microwave Q of BST is worse than the ones obtained with the tuning plates.

II.2 Single Crystal Piezoelectric Actuators

Two different types of single crystal actuators were prototyped and characterized during this period of the project. The first design is called "31" mode flextensional actuator, as shown in Figure 4.

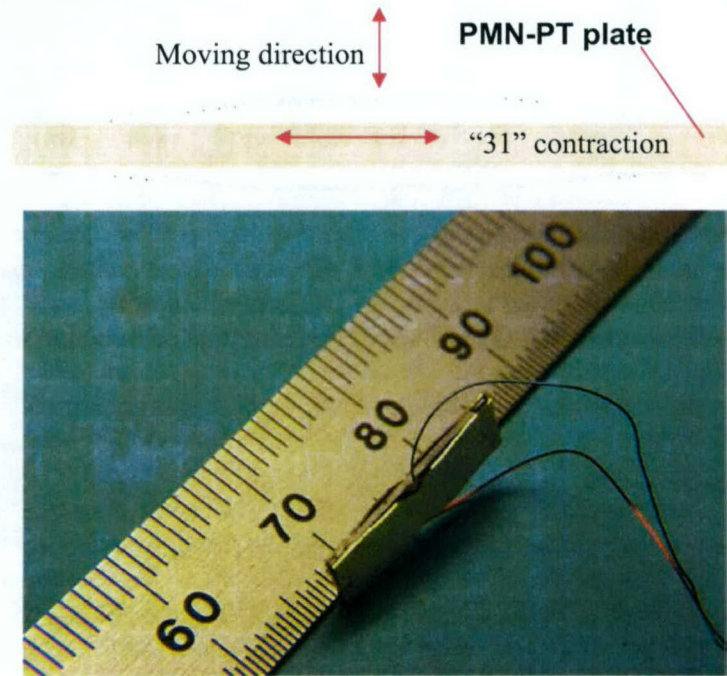
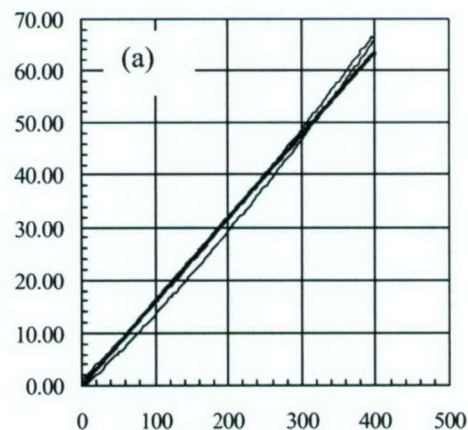


Figure 4. "31" mode single crystal flextensional actuator.

High quality PMN-PT crystal plate with dimension of 15mmx6mmx0.5mm and Cr/Au electrodes was bonded to the two brass endcaps with special design to achieve the large motion amplification. The displacement of this actuator was measured using LVDT system and the displacement vs. electric driving voltage is shown in Figure 5(a). It is seen that over 66 μm stroke was obtained under 400 V (equivalent to field of 8KV/cm), very promising considering such a low profile actuator, though higher stroke ($\sim 100\mu\text{m}$) is expected under 500 V from the modeling. The resonant mode of this actuator is recorded as shown in Figure 5(b), the 7.5 KHz resonant frequency indicates the fast response of this actuator, which is desired in tunable filters.



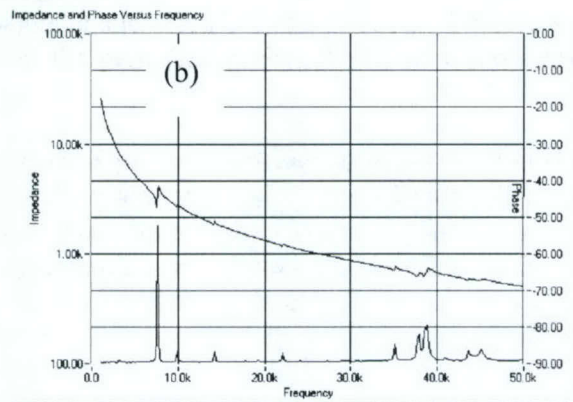


Figure 5. “31” flextensional actuator characterization. (a) displacement vs. driving voltage. (b) impedance and phase of the actuator varies with frequency (resonant modes).

An actuator housing is also designed and prototyped, as shown in Figure 6, to incorporate the actuator with the tuning plate. It is noticed that the single actuator stroke is still relatively low, two such actuators in serial was assembled higher stroke and more than 150 μm was obtained with two actuators in serial, which is large enough for many filter tunings.

The 2nd actuator design is called “33” mode flextensional actuator, where a single crystal stack actuator is inserted into a thin metal frame (amplification mechanism). The frame was provided by Adeptronics and is a standard APA60 frame, not a specially designed one. The PMN-PT stack actuator (Figure 7) consists of 40 layers of PMN-PT plates with dimension of 5mmx5mmx0.5mm. The assembled “33” mode flextensional actuator is shown in Figure 8.

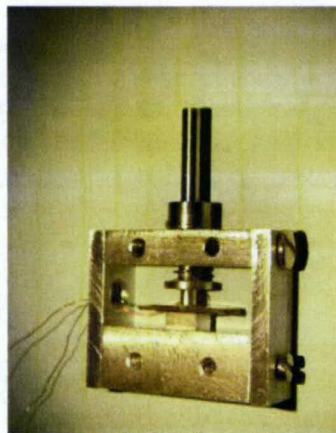


Figure 6. “31” flextensional actuator in a housing.



Figure 7. PMN-PT stack actuator.



Figure 8. Assembled "33" mode flextensional actuator.

The actuator was characterized by measuring the strain vs. field and the resonant modes. Figure 9(a) shows the displacement output of the actuator under various electric driving voltages, $>80 \mu\text{m}$ stroke is achieved under 400 V (or field of 8 kV/cm), and larger than 100 μm is obtained under 500 V. The resonant modes showed that the resonant frequency of this actuator is about 7-9 KHz (Figure 9(b)), indicating fast response in filter tuning.

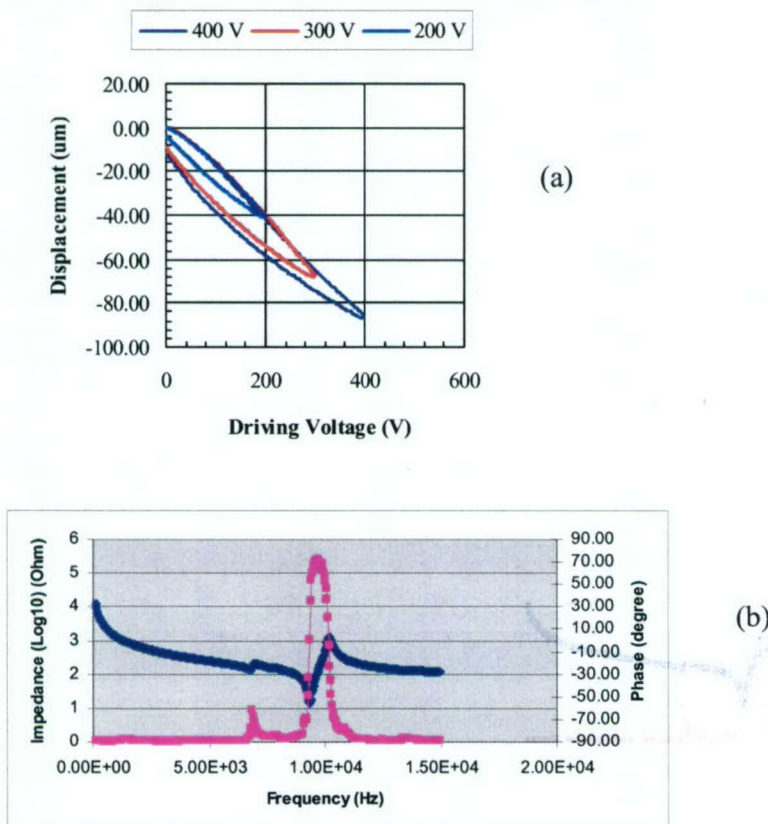


Figure 9. Characterization results for a single crystal "33" mode flextensional actuator. (a) displacement vs. driving voltage; (b) resonant modes: impedance and phase vs. frequency.

In order to achieve larger stroke, two "33" flextensional actuators were connected in serial (as shown in Figure 10(a)) and the displacement is about 218 μm under 500 V

(Figure 10(b)). The cryogenic strain performance of the “33” mode flextensional actuators was measured using LVDT system. The actuator was put in a cryostat chamber with temperature varied from 75K to 300K. The stroke is about 74 μm at 75K under 500V (Figure 11). The displacement of the two actuator in serial at 75K will be around 150 μm , which is promising for HTS filter tuning.

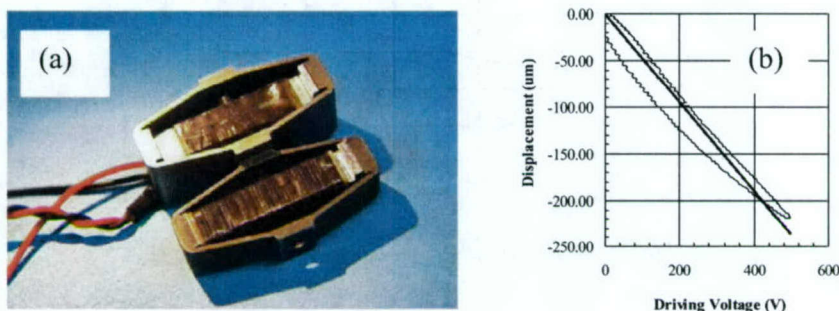


Figure 10. Two “33” flextensional actuator in serial and strain test results. (a) Photograph of the photograph of the two actuators in serial. (b) displacement vs. voltage of the two actuators in serial.

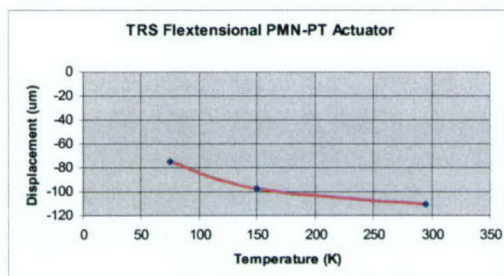


Figure 11. Cryogenic displacement vs. voltage of the “33” flextensional single crystal actuator.

II.3 Piezo Tuned Horseshoe Resonator

A. PRINCIPLE OF OPERATION

We demonstrate feasibility of the piezotuned filters by exploring planar structures based on recently developed dual mode tunable filters [8]. A prototype structure of the horseshoe filter is shown in Figure 12. The offset of the feed lines, characterized by the parameter s in Figure 12, is required to obtain a band-pass and distance h controls coupling strength between individual resonators.



Figure 12. Top view of a resonant horseshoe structure.

The filter is based on magnetically coupled resonators. This coupling takes place in the narrow gap where the magnetic field is at its maximum and electric field is minimum and close to zero. Near the upper and lower edges of each resonator, there is large electric field, and it is this region, which is used in tuning. Plates with relatively high K are positioned above these regions, and effective capacitance is increased by reducing the gap between the resonator and tuning plates. A piezoelectric actuator can rapidly move the tuning plates. The attractiveness of such a filter is that by loading capacitive regions only, its effect on the coupling between resonators is minimized. This permits tuning of the filter with a minimal change of its band-pass characteristics. Also, loading of the filter results in only small changes in impedance resulting in stable filter characteristics while center frequency can be tuned in a wide range.

For the horseshoe structure a commercial LTCC tape with $\epsilon_r = 6$ was used for substrates and commercial conductor paste was used for the electrodes. The diagram of the filter as used in FDTD modeling is shown in Figure 13. The planar filter is shown with two tuning plates placed directly on top of capacitive regions of the filter. The dimensions used were $15 \times 15 \times 0.66 \text{ mm}^3$. All of the salient filter characteristics are maintained as the filter dimensions changed and only the resonant frequency is altered with size. The comparison between FDTD modeling and experimentally measured S_{21} parameters agree well (Figure 14), and the insertion loss is less than 2 dB.

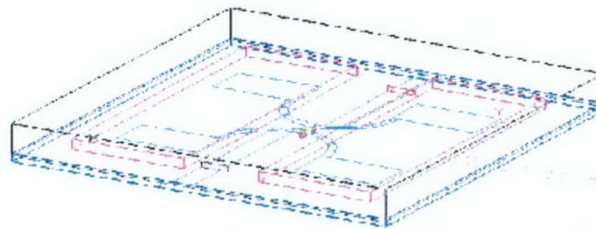


Figure 13. A diagram of the horseshoe resonator with two large tuning dielectric plates on top of capacitive regions.

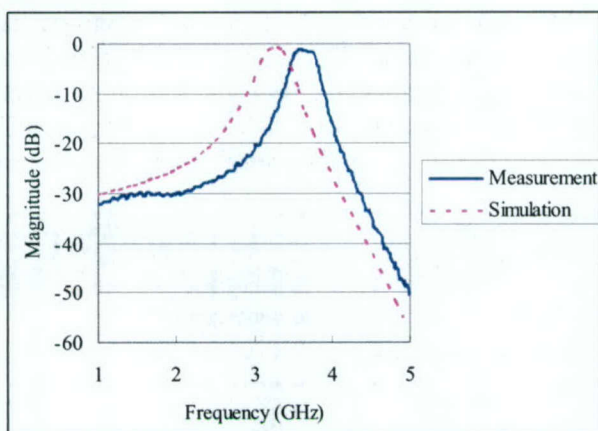


Figure 14. Experimental and simulated data of the horseshoe structure.

Two approaches were used for testing tunabilities of fabricated resonators: 1) a direct placement of tuning plates on top of a resonator, and 2) actuators utilizing piezoelectricity were used for controlled displacement of tuning plates above the resonators.

It was determined that the relative sizes of tuning plate and the capacitive regions of resonators are crucial to obtain high tunability. For the clarification, a schematic drawing is shown in Figure 15 in which tuning plates are the same size (top) and larger (bottom) compared to the capacitive regions of the filter, respectively.

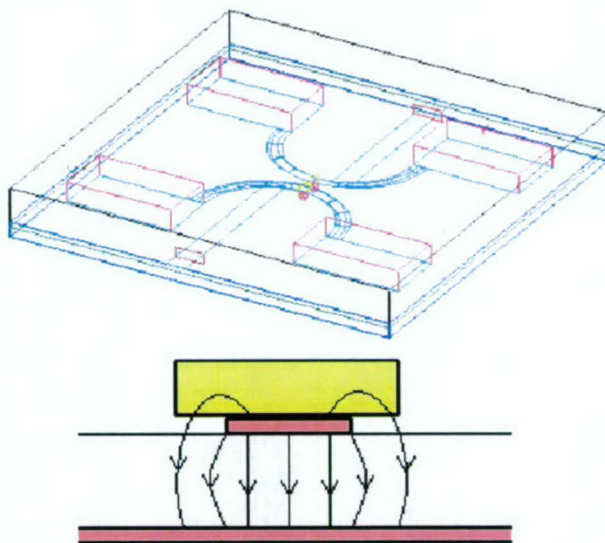


Figure 15. Modeling frame for the filter with tuning plates placed on top of capacitive regions (top) and electric field in microstrip with a dielectric plate (bottom).

One can see from the drawing that stray fields returning to the ground plane have a smaller gap to cross if the tuning plate extends beyond the capacitive region of the filter. When the four tuning plates just covered the capacitive regions of the electrodes, the tunability was in the range of 1-3 %; with two large tuning plates covering two capacitive regions each (Figure 16), the measured tunability was as high as 30%.

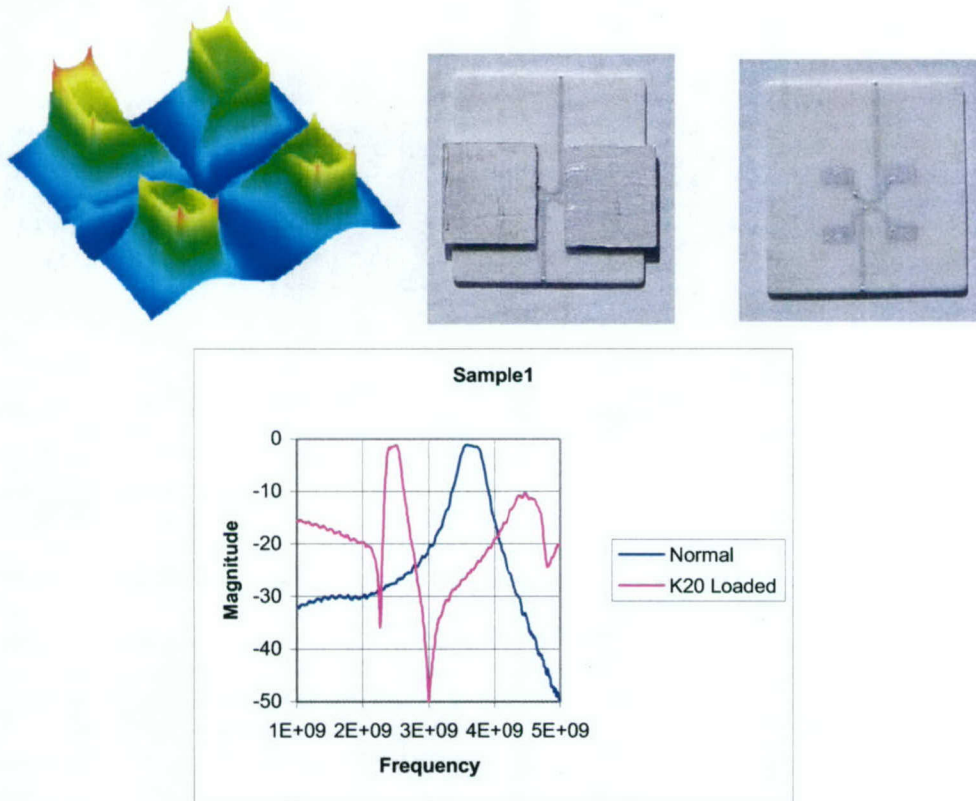


Figure 16. Prototype of the horseshoe structure (top left electric field magnitude, top middle without dielectric; top right: with the dielectric). Bottom: Experimental s_{21} curves for the frequency shift in horseshoe structure as a result of loading with $\epsilon_r = 22$ dielectric.

The effect of different dielectric constant for the loading plates was explored by the FDTD modeling and also experimentally. The model predicts that a higher tunability should be obtained by loading the sample with higher ϵ_r tuning plate. This was also observed experimentally but only up to a point. Experimentally, the best tunability is obtained with moderate dielectric constant in the range of 20 to 40 for the loading plates. It appears that for higher ϵ_r , the impedance mismatch makes it difficult for energy to be channeled into the tuning plate, especially in presence of sample imperfections leading to air gaps for the plate in contact with the resonator. The example of resonator loaded with 2 large plates having dielectric constant = 22, indicates tunability of 30% with insertion loss less than 2 dB. Such good tunability with moderate ϵ_r is encouraging since a number of materials are available that have high Q for this relatively modest dielectric constant.

For the case of four plates extending laterally beyond capacitive region (Figure 15), the effects of dielectric constant of the loading plate on the filter characteristics were modeled with the FDTD. The results are summarized in Figure 17. A similar magnitude of frequency shift is observed for the case of a single large tuning plate covering the whole filter but in that case, insertion loss was increased appreciably for the

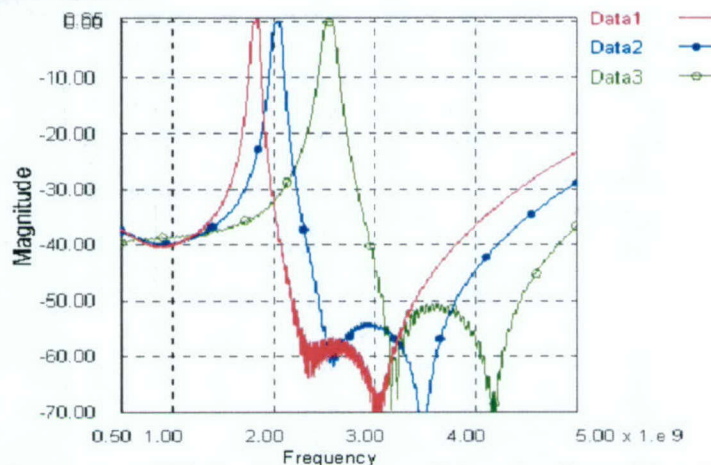


Figure 17. Frequency shift for S_{21} with four dielectric plates (Data1: $\epsilon_r=50$, Data2: $\epsilon_r=20$, Data3: none).

The tunability is a strong function of a distance between tuning plate and the horseshoe filter. The tuning curve becomes very steep for small gap between the tuning plate and the filter. Most of the tuning is achieved for the gap ranging between zero and 200 microns; this displacement range is achievable with the piezoelectric actuators. For the actuators used in this study the fundamental resonance frequency was close to 10 kHz implying a sub millisecond tuning of filter should be achievable. Modeling result for the filter performance as a function of displacement is shown in Figure 18.

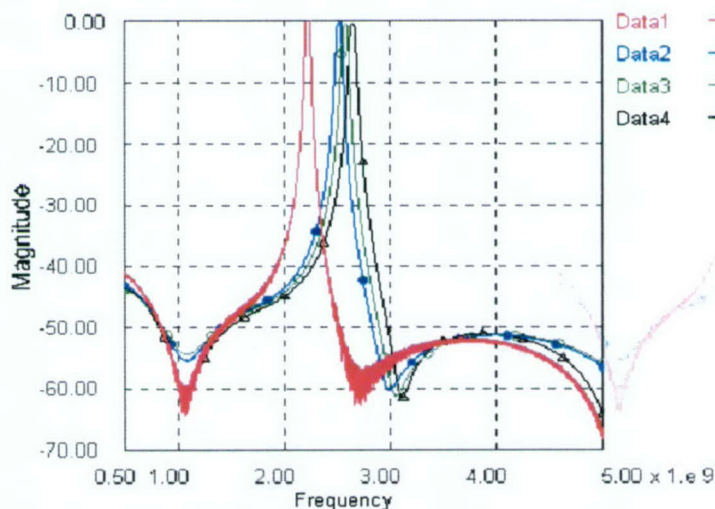


Figure 18. S_{21} parameters with different distances between substrate and dielectrics (Data1: 0mm (contact), Data2: 0.125mm, Data3: 0.250mm, Data4: No dielectrics).

To obtain optimized filter response it is required to get a good alignment between the dielectric tuning plate and the substrate. Once this alignment is achieved, the shape of the filter characteristics and insertion loss do not change appreciably with dc bias applied to the piezoelectric actuator. The tuning setup is shown in Figure 19. The tuning plates was moved almost touching the resonator substrate, and then drive the actuator under voltage of 0V-500V to move the dielectric tuning plates away from the substrate, recording the S_{21} magnitude using the analyzer, Figure 20 shows the tuning results, the

tuning range is about 19% and the insertion loss is much lower ($< 2\text{dB}$) in the case of $k=22$ tuning plate. Filter preserves its shape for different tuning conditions because it is designed to have impedance roughly independent of capacitive loads introduced by piezoelectric tuning.

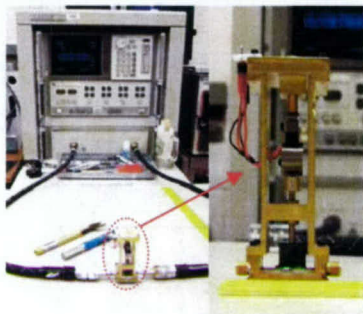


Figure 19. Tuning setup using “33” flextensional actuator.

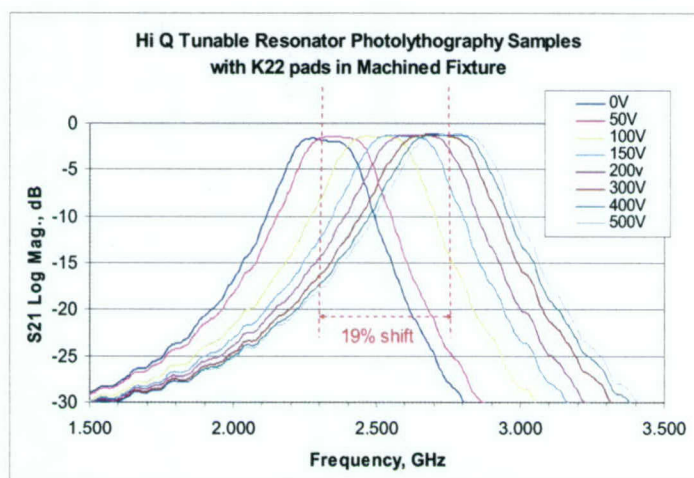


Figure 20. S_{21} parameters with applied voltage in the range of 0 to 500 Volts.

III. Piezo Tuned HTS Resonator

III.1 Dielectric Tuning

The HTS resonator (Figure 21(a)) with YBCO film on MgO substrate provided by STI (Superconductor Technologies, Inc.) was used for cryogenic tuning experiments. The resonant loaded Q of this filter was 10538. Firstly, dielectric tuning using plates with various dielectric constant was carried out by using dielectric tuning plate with dielectric constant of 2-88. The tunability of HTS resonator with different tuning dielectrics was explored by placing these dielectrics on top of the filter and measuring the S_{21} parameters in liquid nitrogen. In Table II a summary of filter response in liquid nitrogen in presence of different tuning dielectric materials with the dielectric constant in the range of 2 to 88 is shown. Interestingly, the highest tunability of 16% was observed for the dielectric with $k = 36$. By comparison, $k = 31$ and $k = 88$ resulted in tunability of

10%. This result is reminiscent of previous observation of maximum tunability for tuning plate with $K = 22$ observed in ring resonators. One possible source of drop off in tunability for high K tuning plates is the strong impedance mismatch between the substrate and tuning plates which leads to difficulty in storing EM energy in the tuning plate. Should reflection from the tuning plate become large, the response will start to resemble that of metal tuning plate, and even a change in sign for tunability may take place, although it was not observed experimentally.

Table II. Filter characteristics with different tuning plates

Material	Material K	Material Q	Resonant Peak Q	Tunability
none			10538	
Teflon	2	2500	7543	1%
Ferro A6	6	1000	7620	5%
Dupont	22	?	1191	7%
Trans-Tech	31	14607	6448	10%
Trans-Tech	36	11118	7674	16%
CTS	88	1667	6767	10%

There is a reduction in measured Q for all dielectric plates tested compared to the filter by itself. There is no simple dependence between the material Q (column 3) and Q of the resonator with the plate made of that material on top (column 4). More surprising, even for the filters with the same tunability, $K = 31$ and $K = 88$, there is no direct dependence of resonant peak Q to material Q suggesting different types of EM interactions in the composite media for strongly different K of tuning plates. Figure 21(b) shows s_{21} peaks for different tuning plates.

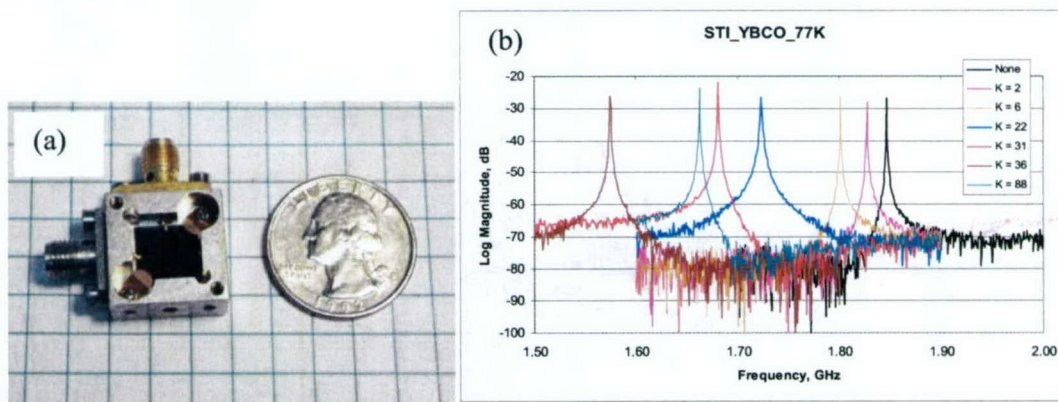


Figure 21. Cryogenic dielectric tuning for HTS filter. (a) HTS resonator from STI; (b) dielectric tuning at 77K.

III.2 Cryogenic Piezo Tuning

The cryogenically compatible two-stage flextensional actuator (Figure 10) was used to tune a highly tunable High-Temperature Superconducting (HTS) electromagnetic resonator designed by STI for its use in tunable filter systems. The actuator by itself is expected to provide approximately 150 to 250-microns of vertical movement at cryogenic temperatures. The actuator was affixed to a micrometer head using thermally compatible epoxy to facilitate cooling. The micrometer head had been previously reconditioned to operate at cryogenic temperatures, and was used in this case to make coarse adjustments in the tuning set-up. An HTS tuning tip was affixed to the free side of the flextensional actuator using the same thermally compatible epoxy. Once the micrometer head was adjusted to pre-position the actuator/tuner assembly near the resonator, the two-stage flextensional actuator was used to make fine-tuning adjustments to the resonator, and the frequency response was measured and recorded.

Two sets of experiments were conducted. In the first set of experiments, the resonator was weakly coupled to the rest of the circuit to see if an accurate measure of the resonator/tuner pair Q could be obtained directly. The tuner height was chosen to demonstrate the maximum tunability achievable with this actuator/resonator/tuner. In this case, the tuner is set relatively close to the substrate such that the sensitivity to tuner movement is a maximum, though the circuit Q is at a minimum. In the second set of experiments, the resonator was closely coupled to the external circuit to obtain a cleaner, more easily measurable response of the resonator/tuner pair.

A. Experimental Set-up

A previously modified cryogenically compatible micrometer head was attached to a base fixture, which extends the actuator/tuner assembly into the cavity of a microwave enclosure sufficiently close to the tunable HTS resonator. We initially tried to mount the set-up in a temperature controllable cryostat, which would have allowed us some more freedom in experimentation, though we were unable to get a proper conduction path sufficient to cool the HTS tuner and maintain adequate temperature stability. It was then decided that the entire set-up would be mounted to a conduction plate and submerged in liquid nitrogen to ensure adequate cooling of all the essential parts. The device was left to settle so the temperature in the experimental set-up would reach equilibrium.

The 0 to 500 volts necessary to drive the actuator was provided by a Sorensen DCR 600-.75B power supply. This power supply has a very limited output resolution and the actual voltage output was monitored using an HP-3478A multimeter.

B. RF Measurements

In the first set of experiments, the resonator was weakly coupled to the rest of the circuit to measure the *unloaded* Q of the resonator/tuner assembly. As can be seen in the first few figures, the measured transmission response is relatively "grassy" due largely to the vibration in the liquid medium, so an accurate measurement of the Q_{UL} was unable to be obtained. However, a rough estimate can be obtained by dividing the resonator frequency (f_0) by the average measured bandwidth 3 dB below the minimum insertion loss point in the transmission response (Figure 22).

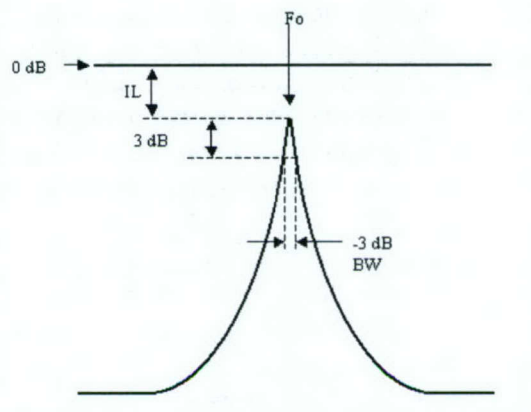


Figure 22. Estimation of unloaded resonator Q.

To begin with, the micrometer head was used to position the tuner/actuator assembly as close to the resonator as possible. This corresponds to the outermost end of the tuning range, i.e. farthest away from the resonator design turn-on frequency and together with the weak coupling explains the high insertion loss. Figures 23 shows a rough glimpse of the tuning ability of the device under test. The measurements were carried out on an Agilent E8358A PNA series vector network analyzer. The turn-on frequency was around 918 MHz at zero applied voltage, and moved about 12 MHz with an applied voltage of 500 VDC. The next series of figures are the actual measured data for five different voltage settings. 0, 100, 200, 300, 400, and 500 VDC. The frequency shifts can be read of the screen and are displayed in the captions. Inspection of the graphs for the weakly coupled device shows an insertion loss greater than -50 dB. This is because the resonator is tuned so far off of its design frequency at this point. The insertion loss will be at a minimum when the resonator is tuned to its design frequency, and a maximum when it is tuned to its farthest point. The overall Q suffers the same fate as the insertion loss with respect to tuning away from the design frequency. In this case, the unloaded Q of this particular resonator at this frequency was estimated to be roughly:

$$Q_{UL} = \frac{f_0}{-3dB BW} \Rightarrow \frac{900 MHz}{0.15 MHz} = 6,000$$

After we warmed up the experiment it was found that the HTS resonator chip had been damaged upon warm-up. A new resonator was mounted and coupled more closely to the rest of the circuit to get a cleaner response. Again, the entire system was completely submerged in liquid nitrogen for rapid and complete cooling. Once the system reached equilibrium the micrometer head was again used to position the tuner/actuator assembly sufficiently close to the resonator to provide the maximum amount of tuning for the given travel distance available with the actuator. Figures 24-25 are the captured transmission scattering parameters using the new set-up. Again the micrometer head was used to position the tuner/actuator assembly near the resonator for maximum tunability. The turn-on frequency was near 902 MHz and, with the actuator fully charged, the frequency

was shifted by nearly 25 MHz. The same voltage increments were used in this experiment, starting at zero and increasing to 500 VDC. The insertion loss at these frequencies measured around -10 dB, which is normal since the resonator is tuned to its most extreme tuning position i.e. farthest away from the design frequency. Careful inspection of the insertion loss measurements might lead one to believe that the insertion loss is improving with increasing voltage. Since the flextensional actuator's dimension in the vertical direction is decreasing with increasing voltage, the resonator is being tuned closer and closer to the design frequency with increasing actuator voltage. Therefore the insertion loss is expected to improve due to the nature of the resonator alone and not as a result of the presence of the actuator.

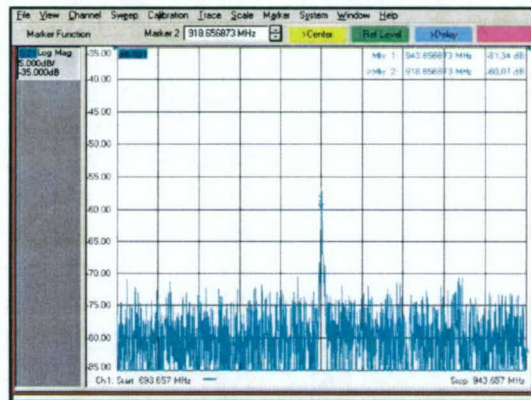


Figure 23. HTS resonator with weak coupling (918 MHz. Voltage = 0).

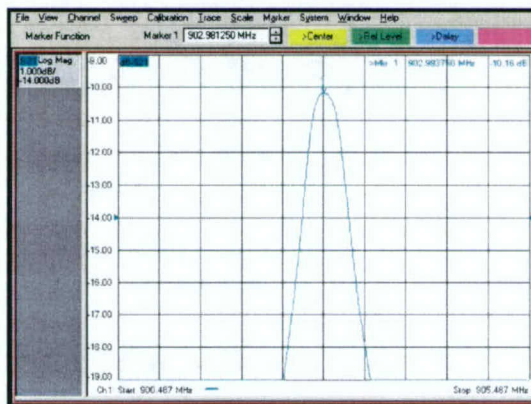


Figure 24. HTS resonator with strong coupling at Voltage = 0 VDC, Freq = 902.994 MHz.

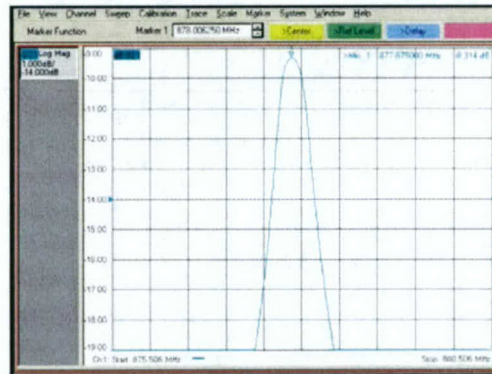


Figure 25. HTS resonator with strong coupling at Voltage = 500 VDC, Freq = 877.875 MHz.

IV. Conclusions

Piezoelectric tuning is shown to be an effective approach to tune microwave filters with **high tunability in the range of 20% and with low insertion losses of less than 3 dB**. Furthermore, the shape of the passband is fairly well preserved despite large tuning range. The horseshoe filter used in this work is especially well adapted to the piezoelectric tuning since the regions for tuning are well separated from the coupling regions of the filter.

The single crystal flextensional piezoelectric actuators show large stroke (>150 μm) at cryogenic temperature (77K) and with low profile. The actuator exhibited significantly more travel than other similar polycrystalline piezoelectric actuators at these extreme temperatures. **With this flextensional actuator (150 μm stroke at 77K), STI HTS resonator was tuned about 25 MHz or about 3% without any coarse adjustments and Q of > 6000 (original value of 10,000) at 77K.**

Acknowledgement

The authors would like to thank Hua Lei at TRS for actuator assembly assistance, Eric Prophet from STI for cryogenic tuning experiments.

References

- [1] T.-Y. Yun and K. Chang, "Piezoelectric-transducer-controlled tunable microwave circuits," *IEEE Trans. Microwave Theory & Tech.*, vol.50, no. 5, pp.1303-1310, May 2002.
- [2] L.-H. Hsieh and K. Chang, "Piezoelectric Transducer tuned bandstop filter," *Electronic Letters*, vol. 38, no. 17, pp. 970-971, 2002.
- [3] J. Tao, B. Chan, H. Baudrand, J. Ateghian, "Novel type of electrically-controlled phase shifter for millimeter-wave use: theory and experiment," *1991 MTT-S Int. Microwave Symp. Digest*, pp. 671-674, 1991.

- [4] Y. Poplavko, Y. Prokopenko, V. Molchanov, and A. Dogan, "Frequency-tunable Microwave dielectric resonator," *IEEE Trans. Microwave Theory & Tech.*, vol.49, no. 6, pp.1020-1026, June 2001.
- [5] S.E. Park and T. Shrout, "Relaxor Based Ferroelectric Single Crystals for Electro-mechanical Actuators", *Mat. Res. Innovat.*, **1**, pp. 20-25, 1997.
- [6] D. S. Paik, S. E. Park, W. S. Hackenberger, and T. R. Shrout, "Dielectric and Piezoelectric Properties of Perovskite Materials at Cryogenic Temperatures", *J. Mat. Sci*, **34**, pp. 469-473 (1998).
- [7] D. Oates and G. Deonne, "Magnetically Tunable Superconducting Resonators and Filters," *IEEE Trans. On Appl. Superconductivity*, Vol. 9, no. 2, pp. 4170 – 4175.
- [8] A. Hennings, G. Semouchkin, E. Semouchkina, and M. Lanagan, "Design Optimization of Microstrip Square-Ring Band-Pass filter with Quazi-Elliptic Function," 33rd European Microwave Conference.